Earth Science Faculty Scholarship

Earth Sciences

3-8-2008

Magma-Driven Multiple Dike Propagation and Fracture Toughness of Crustal Rocks

Z.-H. Jin

Scott E. Johnson
University of Maine - Main, johnsons@maine.edu

Magma-driven multiple dike propagation and fracture toughness of crustal rocks

Z.-H. Jin[1] and S. E. Johnson[2]

[1]   Dike swarms consisting of tens to thousands of subparallel dikes are commonly observed at Earth's surface, raising the possibility of simultaneous propagation of two or more dikes at various stages of a swarm's development. The behavior of multiple propagating dikes differs from that of a single dike owing to the interacting stress fields associated with each dike. We analyze an array of parallel, periodically spaced dikes that grow simultaneously from an overpressured source into a semi-infinite, linear elastic host rock. To simplify the analysis, we assume steady state (constant velocity) magma flow and dike propagation. We use a perturbation method to analyze the coupled, nonlinear problem of multiple dike propagation and magma transport. The stress intensity factor at the dike tips and the opening displacements of the dike surfaces are calculated. The numerical results show that dike spacing has a profound effect on the behavior of dike propagation. The stress intensity factors at the tips of parallel dikes decrease with a decrease in dike spacing and are significantly smaller than that for a single dike with the same length. The reduced stress intensity factor indicates that, compared to a single dike, propagation of parallel dikes is more likely to be arrested under otherwise the same conditions. It also implies that fracture toughness of the host rock in a high confining pressure environment may not be as high as inferred from the propagation of a single dike. Our numerical results suggest fracture toughness values on the order of 100 MPa $\sqrt{m}$. The opening displacements for parallel dikes are smaller than that for a single dike, which results in higher magma pressure gradients in parallel dikes and lower flux of magma transport.

1. Introduction

[2]   It is well-known that magma transport via dike propagation is a principal mechanism for magma ascent, significantly influencing the geological evolution of Earth's crust and volcanism on Earth's surface [e.g., *Halls and Fahrig*, 1987; *Pollard*, 1987; *Spence et al.*, 1987; *Clemens and Mawer*, 1992; *Rubin*, 1995a; *Ernst et al.*, 2005; *Gudmundsson*, 2006]. Dikes initiate from magma source regions that can vary in size from a small magma chamber feeding an overlying volcano [e.g., *Segall et al.*, 2001; *Wright and Klein*, 2006] to a broad zone of partial melting hundreds of kilometers across [e.g., *Kelemen et al.*, 1997; *Nakajima et al.*, 2001; *Guernina and Sawyer*, 2003; *Unsworth et al.*, 2005].

[3]   Although the mechanisms of dike initiation are not well understood, initiation sites are likely to be controlled by small-scale mechanical or physical heterogeneities, such as microstructural defects, local shear strain rate gradients, melt pressure gradients generated by tectonic strains or volume changes associated with melting reactions, to name a few. Given the many different environments from which magma can be sourced, and the large range in length scales for source areas, we expect that multiple dike initiation and propagation from single source regions will occur. We offer several lines of support for this possibility. First, simultaneous multiple cracking has a sound foundation in the physics of materials. For example, ceramics and glasses when subjected to thermal gradients commonly undergo simultaneous, multiple cracking with both stable and dynamic fracture propagation [*Geyer and Nemat-Nasser*, 1982; *Bahr et al.*, 1986; *Wachtman*, 1996]. Second, dike-growth simulation experiments using gelatin and silicone showed that simultaneous nucleation and growth of dikes occurred around the margins of a pressured chamber [*Canon-Tapia and Merle*, 2006]. Third, there is a large body of literature documenting the occurrence of tens to thousands of subparallel dikes and/or melt veins across a wide range of environments and scales, including: (a) individual volcano flanks [e.g., *Walker*, 1986]; (b) subvolcanic magma transport systems [e.g., *Johnson et al.*, 1999]; (c) large subcrustal magma reservoirs such as

---

[1]Department of Mechanical Engineering, University of Maine, Orono, Maine, USA.
[2]Department of Earth Sciences, University of Maine, Orono, Maine, USA.

those in Iceland [e.g., *Gudmundsson*, 1990, 1995]; (d) ophiolites that formed at mid-ocean ridges [e.g., *Nicolas et al.*, 1994]; (e) dike swarms associated with large igneous provinces like the Deccan Traps [e.g., *Ray et al.*, 2007]; (f) arrays of giant mantle-sourced dikes [e.g., *Ernst et al.*, 2001]; and (g) vast exposed areas of once partially molten lower to middle continental crust [e.g., *Guernina and Sawyer*, 2003]. The occurrence of multiple, subparallel dikes in these exposed environments is not necessarily evidence for simultaneous multiple dike propagation. However, simultaneous initiation and propagation cannot be ruled out, leading us to question how multiple dikes interact with one another, how this interaction might affect magma transport, and what the implications are for the material properties, such as fracture toughness, of crustal rocks.

[4] Although progress has been made in understanding magma transport via dike propagation, published investigations have been focused primarily on the propagation of a single dike [*Weertman*, 1971; *Secor and Pollard*, 1975; *Spence and Sharp*, 1985; *Spence et al.*, 1987; *Lister*, 1990, 1991, 1994a, 1994b; *Lister and Kerr*, 1991; *Rubin*, 1993, 1995a, 1995b, 1998; *Parfitt and Head*, 1993; *Bonafede and Olivieri*, 1995; *Bonafede and Rivalta*, 1999; *Fialko and Rubin*, 1998; *Meriaux and Jaupart*, 1998; *Bolchover and Lister*, 1999; *Ida*, 1999; *McLeod and Tait*, 1999; *Meriaux et al.*, 1999; *Dahm*, 2000a, 2000b; *Menand and Tait*, 2002; *Kuhn and Dahm*, 2004; *Roper and Lister*, 2005; *Rivalta and Dahm*, 2006; *Chen et al.*, 2007]. In addition to these investigations, a few analog and numerical studies have explored the interaction of multiple dikes. *Takada* [1989] considered the propagation of a system of parallel dikes using a numerical model. He used both conventional tensile strength and fracture mechanics criteria to determine dike arrest near the level of neutral buoyancy. Magma flow was apparently not considered in the model. *Takada* [1994] used liquid-filled fractures in gelatin to investigate experimentally the interactions of both collinear and parallel multiple dikes. He observed that lower remote differential stresses promote the coalescence of parallel dikes. *Ito and Martel* [2002] attempted to identify the controlling parameters of dike interaction using experiments with liquid-filled fractures in gelatin, combined with numerical modeling. They found that in a cluster of multiple parallel dikes with different heights, individual dikes propagate following different paths. The adjacent dikes merged or deviated from one another depending on their interactions. The remote differential stress, dike driving pressure, dike spacing and the size of dike head all influenced the dike interactions. Using a numerical model, *Kuhn and Dahm* [2004] analyzed the effect of dike interaction and differential stress on the migration path and dike arrest.

[5] In this paper, we investigate the effects of dike interactions on dike propagation behavior and associated magma transport, and implications for the magnitude of fracture toughness in crustal rocks. This problem involves nonlinear coupling of solid mechanics, fracture mechanics and fluid mechanics, necessitating a relatively simple geometrical configuration in order to obtain a semi-analytical solution. Using a perturbation method that we recently developed [*Chen et al.*, 2007] for the low velocity (e.g., less than 0.5 m/s) propagation of a single dike filled with low viscosity magma (e.g., less than 100 Pa-s), we analyze an array of parallel, periodically spaced dikes that grow simultaneously from an overpressured source into a semi-infinite host rock. Although the parallel dikes observed in many localities on Earth and other planets may be injected separately at different times, the possibility of simultaneous injection cannot be excluded, as discussed above. Despite the geometrical simplifications of our model, the solution represents an important step in our understanding of multiple dike interaction and magma transport, and our perturbation method provides a new pathway for semi-analytical treatment of the problem. The present work assumes steady state (constant velocity) magma flow and dike propagation, which approximates some stages of the time-dependent propagation process [*Spence et al.*, 1987; *Lister*, 1991]. Moreover, the steady state solution is sufficient for the purpose of estimating the upper limit of fracture toughness [*Anderson*, 1991].

[6] The remainder of this paper is organized as follows. Section 2 reviews the fluid mechanics equations for magma flow within dikes. Section 3 describes the fracture mechanics formulations for the periodic dikes and the perturbation technique to solve the coupled nonlinear problem. In section 4, we present numerical examples to illustrate the effects of different dike spacing on the dike-tip stress intensity factors and dike surface profiles. Section 5 discusses the implications of the model solution for the magnitude of fracture toughness in crustal rocks. Finally, section 6 provides concluding remarks.

2. Fluid Mechanics Model of Magma Transport

[7] Consider an array of parallel dikes that propagate vertically from a magma source into a semi-infinite host rock (Figure 1). We assume that the dikes are periodically located with a spacing of H and a length of *a*. The dikes are modeled as magma filled, plane strain edge cracks in a half plane, as shown in Figure 1. The lubrication theory of fluid mechanics has been used to describe magma flow in a single dike [*Spence et al.*, 1987; *Lister and Kerr*, 1991; *Rubin*, 1995a]. For magma transport in parallel dikes, the lubrication theory may still be applicable because the flow in individual dikes does not interact directly. However, the magma flow behavior in parallel dikes may differ from that for a single dike because the dike surface openings are affected by the elastic deformation interactions among the dikes.

[8] In lubrication theory, the magma flux q and pressure p follow the relationship of Poiseuille flow [*Panton*, 1984]

$$q = -\frac{\delta^3}{12\eta}\frac{\partial}{\partial Z}(p + \rho_m g Z) \qquad (1)$$

where η denotes the magma viscosity, ρ_m the magma density, δ the opening displacement of the two dike surfaces, g the gravitational acceleration, and Z the vertical coordinate. The continuity equation is

$$\frac{\partial \delta}{\partial t} = -\frac{\partial q}{\partial Z} \qquad (2)$$
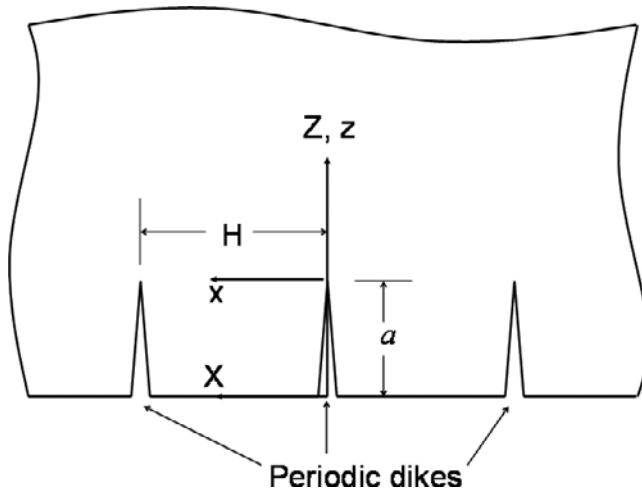
Figure 1. Propagation of an array of parallel dikes into a semi-infinite space.

where t is time. Substituting equation (2) into equation (1) yields

$$\frac{\partial \delta}{\partial t} = \frac{1}{12\eta} \frac{\partial}{\partial Z} \left[\delta^3 \frac{\partial}{\partial Z} (p + \rho_m g Z) \right] \quad (3)$$

[9] Under steady state magma flow conditions, i.e.,

$$\frac{d}{dt} = -V \frac{\partial}{\partial z} \quad (4)$$

where $z = Z - a$ is the moving coordinate centered at the moving dike tip and V is the dike propagation velocity, equation (3) becomes

$$-V \frac{\partial \delta}{\partial z} = \frac{1}{12\eta} \frac{\partial}{\partial z} \left[\delta^3 \frac{\partial}{\partial z} (p + \rho_m g(z + a)) \right] \quad (5)$$

in the moving coordinate system. The pressure, p_e, due to the elastic deformation of the host rock can thus be obtained as

$$p_e = p + \rho_{eff} g Z = \Delta P + \Delta \rho g(z + a) - 12\eta V \int_{-a}^{z} \delta^{-2} dz \quad (6)$$

where ΔP is the overpressure at the dike base $z = -a$ ($Z = 0$) and $\Delta \rho = \rho_{eff} - \rho_m$ with ρ_{eff} being an effective (or modified) rock density introduced by *Roper and Lister* [2005]

$$\rho_{eff} g = \frac{d}{dZ} (\rho_s g Z + \Delta \sigma) \quad (7)$$

in which $\Delta \sigma$ is the tectonic stress perpendicular to the dike plane [*Rubin*,1995a; *Roper and Lister*, 2005] and ρ_s the density of the host rock.

[10] Here we assume a constant overpressure at the base of the dike [*Rubin*, 1995a], which may be approximately applicable if the amount of magma transported by the dikes represents a small fraction of magma in the overpressured source region. The overpressure, however, decays with time if a substantial portion of the magma in the overpressured source region is evacuated [*Parfitt and Head*, 1993; *Yamaoka et al.*, 2005].

3. Fracture Mechanics Formulation of Parallel Dikes

[11] Periodic edge cracking in an elastic half plane was studied by *Benthem and Koiter* [1973] and *Nied* [1987]. Here we use a singular integral equation method that is similar to the one employed by *Nied* [1987], which is convenient for coupling the magma flow into the fracture mechanics formulation. Because the dike propagation velocity is much smaller than the wave speed of the host rock, the inertia effect can be ignored and the problem becomes quasi-static. The final singular integral equation for the parallel, plane-strain edge-crack problem of a semi-infinite space is derived as follows

$$\int_{-a}^{0} \left[\frac{1}{z' - z} + k_1(z, z') + k_2(z, z') \right] \varphi(z') dz' = \frac{2\pi(1 - \nu^2)}{E} p_e(z),$$
$$- a \leq z \leq 0 \quad (8)$$

where E is Young's modulus, ν is Poisson's ratio, $\varphi(z)$ is the dislocation density function defined by

$$\varphi(z) = \frac{\partial u_x}{\partial z} \Big|_{x=0} = \frac{1}{2} \frac{\partial \delta}{\partial z} \quad (9)$$

with $u_x(z, x)$ being the displacement perpendicular to the crack, and $k_1(z, z')$ and $k_2(z, z')$ are known kernels given by

$$k_1(z, z') = \frac{1}{z + z' + 2a} - \frac{2(z' + a)}{(z + z' + 2a)^2} + \frac{4(z + a)(z' + a)}{(z + z' + 2a)^3} \quad (10)$$

and

$$k_2(z, z') = \sum_{k=1}^{\infty} \left\{ \frac{2(z' - z)}{(Hk)^2 + (z - z')^2} + \frac{4(z' - z)(Hk)^2}{\left[(Hk)^2 + (z - z')^2 \right]^2} \right\}$$
$$- \sum_{k=1}^{\infty} \left\{ \frac{4(z' + z + 2a)}{(Hk)^2 + (z + z' + 2a)^2} \right.$$
$$+ \left. \frac{2(3z' + z + 4a)\left[(z + z' + 2a)^2 - (Hk)^2 \right]}{\left[(Hk)^2 + (z + z' + 2a)^2 \right]^2} \right\}$$
$$+ \sum_{k=1}^{\infty} \frac{8(z' + a)(z + a)\left[(z + z' + 2a)^3 - 3(z + z' + 2a)(Hk)^2 \right]}{\left[(Hk)^2 + (z + z' + 2a)^2 \right]^3}$$
$$(11)$$

respectively, where H is the dike spacing.

[12] We assume that a cohesive zone lies ahead of the dike tip and that this zone is much smaller than the dike length so that the classical linear elastic fracture mechanics (stress intensity factor theory) can be used to study the dike propagation. Under these conditions, the critical Griffith energy release rate equals the intrinsic Griffith energy release rate of the host rock plus the cohesive energy density that describes the energy dissipation in the damage zone around the dike tip. In the same spirit of the small damage

zone, the crack tip cavity may also be ignored if the cavity zone is much smaller than the dike length.

[13] Substituting the elastic pressure in equation (6) into the integral equation (8), we obtain the nonlinear, singular integral equation for the coupled magma flow/parallel dike propagation problem

$$
\int_{-1}^{1}\left[\frac{1}{s-r}+\frac{a}{2}K_1(r,s)+\frac{a}{2}K_2(r,s)\right]\varphi(s)\mathrm{d}s=\frac{2\pi(1-\nu^2)}{E}
$$

$$
\cdot\left\{\Delta P+\Delta\rho g\frac{a}{2}(1+r)-6a\eta V\int_{-1}^{r}\delta^{-2}ds\right\},\quad |r|\leq 1 \quad (12)
$$

where r and s are related to z and z' by

$$
z=\frac{a}{2}(-1+r),\quad z'=\frac{a}{2}(-1+s) \quad (13)
$$

$K_1(r,s)=k_1(z,z')$ and $K_2(r,s)=k_2(z,z')$.

[14] In general, the density of the host rock gradually increases with depth due to compositional changes and pressure gradient. The density difference $\Delta\rho$ thus decreases from a value at the dike base ($z=-a$) with increasing upward distance from the magma source. A power law variation of density is adopted as follows

$$
\Delta\rho=\Delta\rho_0(1-Z/L)^n=\Delta\rho_0(1-(z+a)/L)^n \quad (14)
$$

where $\Delta\rho_0$ is the density difference at the dike base ($Z=0$), L denotes the distance between the dike base and the level of neutral buoyancy and n is the exponent. With appropriately selected L and n, equation (14) approximately describes the density – depth relation reported by *Ryan* [1994].

[15] Equation (12) is a nonlinear integral equation for the dislocation density function $\varphi(r)$. Here we employ a perturbation method [*Chen et al.*, 2007] to attack the nonlinear problem. In the perturbation method, the nonlinear equation (12) reduces to the following series of linear integral equations

$$
\int_{-1}^{1}\left[\frac{1}{s-r}+\frac{a}{2}K_1(r,s)+\frac{a}{2}K_2(r,s)\right]\tilde\varphi_0(s)ds=-\frac{2\pi}{\Delta\rho_0 ga}\Delta P
$$
$$
-\pi(1+r)\left(1-\frac{1+r}{2}\frac{a}{L}\right)^n,
$$

$$
\int_{-1}^{1}\left[\frac{1}{s-r}+\frac{a}{2}K_1(r,s)+\frac{a}{2}K_2(r,s)\right]\tilde\varphi_1(s)ds=\pi S_b^2\int_{-1}^{r}\left(\frac{D}{\tilde\delta_0}\right)^2 ds
$$

$$
\int_{-1}^{1}\left[\frac{1}{s-r}+\frac{a}{2}K_1(r,s)+\frac{a}{2}K_2(r,s)\right]\tilde\varphi_2(s)ds
$$
$$
=\pi S_b^2\int_{-1}^{r}\left(-2\frac{\tilde\delta_1}{\tilde\delta_0}\right)\left(\frac{D}{\tilde\delta_0}\right)^2 ds
$$

$$
\int_{-1}^{1}\left[\frac{1}{s-r}+\frac{a}{2}K_1(r,s)+\frac{a}{2}K_2(r,s)\right]\tilde\varphi_3(s)ds
$$
$$
=\pi S_b^2\int_{-1}^{r}\left(3\frac{\tilde\delta_1^2}{\tilde\delta_0^2}-2\frac{\tilde\delta_2}{\tilde\delta_0}\right)\left(\frac{D}{\tilde\delta_0}\right)^2 ds \quad (15)
$$

with the density function $\varphi(r)$ given by

$$
\varphi(r)=\tilde\varphi(r)\frac{1-\nu^2}{E}\Delta\rho_0 ga
$$
$$
=\frac{1-\nu^2}{E}\Delta\rho_0 ga\left[\tilde\varphi_0(r)+\varepsilon\tilde\varphi_1(r)+\varepsilon^2\tilde\varphi_2(r)+\varepsilon^3\tilde\varphi_3(r)\right] \quad (16)
$$

where ε is a perturbation parameter defined as

$$
\varepsilon=\frac{12\eta\tilde V}{D^2}\frac{1}{\Delta\rho_0 g} \quad (17)
$$

in which D is a parameter with an order of the dike base thickness. In equation (15), the parameter S_b is

$$
S_b=\frac{E}{(1-\nu^2)\Delta\rho_0 ga}
$$

[16] The stress intensity factor, K_I, at the dike tips can be calculated from

$$
K_I=-\frac{\Delta\rho_0 ga\sqrt{\pi a}}{2}\left[\tilde\psi_0(1)+\varepsilon\tilde\psi_1(1)+\varepsilon^2\tilde\psi_2(1)+\varepsilon^3\tilde\psi_3(1)\right] \quad (18)
$$

where $\tilde\psi_i(r)$ ($i=0,1,2,3$) are given by

$$
\tilde\psi_i(r)=\sqrt{1-r}\tilde\varphi_i(r),\quad i=0,1,2,3 \quad (19)
$$

Besides the stress intensity factor, the dike surface opening displacement is also an important physical quantity, which can be calculated from

$$
\delta(r)=\tilde\delta(r)\frac{1-\nu^2}{E}
$$
$$
=\frac{1-\nu^2}{E}\Delta\rho_0 ga\left[\tilde\delta_0(r)+\varepsilon\tilde\delta_1(r)+\varepsilon^2\tilde\delta_2(r)+\varepsilon^3\tilde\delta_3(r)\right] \quad (20)
$$

with

$$
\tilde\delta_i(r)=-a\int_{r}^{1}\tilde\varphi_i(s)ds,\quad i=0,1,2,3 \quad (21)
$$

The convergence of the perturbation series (18) requires that the perturbation parameter ε in equation (17) be small. For some magma flow and dike propagation problems, ε is small enough for convergence. For example, $\varepsilon=0.02$ for mafic dike propagation with typical values of D = 1 m, $\Delta\rho_0=300$ kg/m^3, g = 10 m/s^2, $\eta=50$ Pa-s, and V = 0.1 m/s. Generally speaking, for basaltic magma with a viscosity around 50 Pa-s, the perturbation series converges rapidly and the first two or three terms provide satisfactory results when the dike propagation velocity is lower than 0.1 m/s.

[17] In the present fracture mechanics analyses of multiple dike propagation, we adopt the following three assumptions: (i) steady state dike propagation and magma flow prevail, (ii) the propagation velocity is known a priori, and (iii) dikes are parallel, equally spaced and of the same length. Magma flow and dike propagation are generally
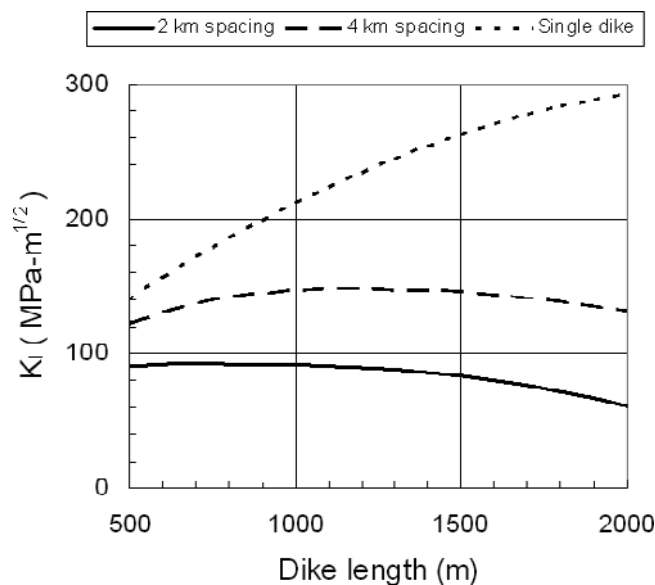
Figure 2. The stress intensity factor versus dike length when the magma source region is 2 km below the LNB (V = 0.01 m/s, $\Delta\rho_0$ = 120 kg/m^3).

transient processes during which the dike propagation velocity is time-dependent and should be determined using the dike propagation condition that $K_I = K_{Ic}$, where K_{Ic} is the fracture toughness of the host rock. Nevertheless, a solution based on the first two assumptions may be approximately applicable to specific stages of dike propagation during which the effects of density gradation and overpressured source trade off and the calculated stress intensity factor remains constant. Moreover, the steady state solution may be employed to delineate the effect of dike spacing on the dike propagation and magma transport behavior and may also be used to estimate the order of magnitude of fracture toughness of crustal rock in a confining pressure environment. The third assumption is made for the convenience of mathematical analysis, but is consistent with many field observations [e.g., *Nicolas et al.*, 1994; *Ray et al.*, 2007]. As discussed previously, parallel dikes that have different lengths and uneven spacing may converge, diverge or arrest owing to interaction with one another.

4. Numerical Results

[18] This section presents numerical examples to illustrate the effect of dike spacing on the stress intensity factor and dike surface profile. Because the main purposes of the present study are to explore the dike interaction effects on dike propagation and the implications for the fracture toughness of crustal rocks, we perform parametric studies based on realistic rock and magma properties and some related field data. In all calculations, we use the following typical properties for the host rock and basaltic magma [*Rubin*, 1995a]: E = 50 GPa, ν = 0.25, η = 50 Pa-s and g = 9.8 m/s^2. The overpressure is taken as ΔP = 3.0 MPa, on the lower end of calculated overpressures for dikes in Iceland [*Gudmundsson*, 1983], Sudan [*Babiker and Gudmundsson*, 2004] and the Deccan Traps of India [*Ray et al.*, 2007]. The density gradation is included with n = 1 and L = 5 km in

equation (14). *Ryan* [1994] has reported the in situ density-depth relations for the East Pacific Rise which may be approximately described by equation (14) with the above n and L. We assume that equation (14) with with n = 1 and L = 5 km may represent some typical density variations in oceanic crust.

[19] Figure 2 shows the stress intensity factor, K_I, versus dike length in the range of 500 m to 2000 m for two values of dike spacing: H = 2 km and 4 km and a dike propagation velocity is taken as V = 0.01 m/s. The result for a single dike is also included. The dike spacing of 2 km is based on the measured dike patterns and trajectories in the Oman ophiolite [*Nicolas et al.*, 1994]. The 4 km spacing dikes and the single dike are included for comparison. The magma source region is assumed to be 2 km below the level of neutral buoyancy (LNB) at which the magma density equals that of the host rock. The density difference $\Delta\rho_0$ at the dike base is assumed as 120 kg/m^3 and our assumed linear density variation leads to a difference of 300 kg/m^3 at a distance of 5 km below the LNB. As no definite information about the position of magma source region is available, a parametric study method is employed. Figure 2 shows that the stress intensity factors for parallel dikes at a given dike length are significantly lower than that for a single dike. For example, the peak values of K_I are 92 MPa $\sqrt{m}$ and 148 MPa $\sqrt{m}$ for the parallel dikes with spacing of 2 km and 4 km, respectively. In contrast, the peak K_I for the single dike is about 293 MPa $\sqrt{m}$ in the dike propagation range considered.

[20] We note that the stress intensity factor remains constant only at some stages of dike propagation. For example, K_I is nearly a constant of about 90 MPa $\sqrt{m}$ over a range of dike length from 500 m to 1200 m for the parallel dikes with a spacing of 2 km. For the case of an increased dike spacing of 4 km, K_I remains nearly constant but the value is about 146 MPa $\sqrt{m}$ over a range of dike length from 900 m to 1500 m. These results demonstrate that steady state propagation may be achieved when the dike has propagated into the vicinity of the LNB. We note that the steady state solution would predict a different response from that of a complete transient model when K_I changes with dike length, but would merge with the transient model when K_I enters a flat region. Furthermore, the steady state stress intensity factor at a growing dike tip represents the maximum effective fracture toughness of the host rock, providing valuable information about the fracture strength of crustal rocks.

[21] Figure 3 shows the dike surface profiles when the dike has propagated 2 km. The physical parameters used in the calculation are the same as those in Figure 2. Whereas the dike surface opening displacement (dike thickness) increases monotonically with the distance from the dike tip for the single dike at the given dike length, the opening for multiple dikes spaced 2 km apart first increases with distance from the tip, reaches a peak value, and then decreases toward the dike base. In addition, multiple dikes are significantly thinner than the single dike. For example, the thickness at the base (z = −2 km) of the single dike is about 0.74 m but the corresponding thicknesses for multiple dikes are about 0.12 m and 0.28 m when the spacing is 2 km and 4 km, respectively. Using the dike surface profile results, the dike surface area (or volume per unit dike width)
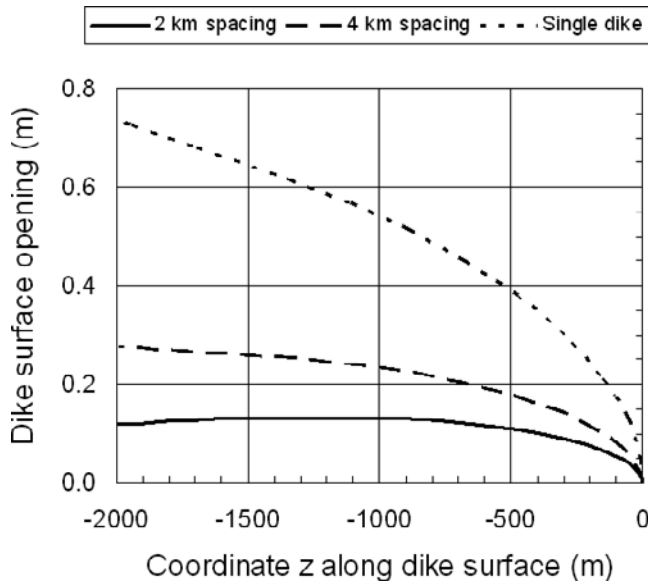
Figure 3. The dike surface opening displacement when the magma source region is 2 km below the LNB (V = 0.01 m/s, $\Delta\rho_0$ = 120 kg/m³).

Figure 4. The stress intensity factor versus dike length when the magma source region is 3.5 km below the LNB (V = 0.01 m/s, $\Delta\rho_0$ = 210 kg/m³).

is approximately calculated as 1010 m² for the single dike, whereas the area reduces to 228 m² for an individual dike in the multiple dike system with 2 km spacing. While this estimate does not consider the transient nature of dike propagation, it indicates that multiple dike interactions significantly reduce the flux of magma transport through dikes.

[22] At the beginning of section 2, we mentioned that the magma flow behavior in multiple dikes may be different from that for a single dike due to the elastic deformation interactions. The elastic interactions of multiple dikes result in narrower dikes. This reduced dike thickness implies that the magma pressure on the dike surfaces will decrease according to equation (6) if the flow velocity remains the same. This conversely will also affect the elastic pressure and the stress intensity factor.

[23] Figures 4 and 5 show the stress intensity factor versus dike length and the dike surface profiles, respectively, for the dikes that have grown to the LNB. The magma source region is now assumed to be 3.5 km below the LNB. The density difference $\Delta\rho_0$ at the dike base is 210 kg/m³. In addition to the dike spacing of 2 km, we also include the results for dike spacings of 3.5 km and 7 km, and a single dike for illustration purposes. The other parameters remain the same as those in Figures 2 and 3. The trends in stress intensity factor and dike surface displacement are similar to those shown in Figures 2 and 3, respectively. The stress intensity factors become larger because of the longer dike length and the higher buoyancy force. For example, the peak K_I value for the 2 km spacing multiple dikes is about 132 MPa $\sqrt{m}$. The corresponding K_I values for the 3.5 and 7 km spacing dikes, and the single dike are about 187, 266 and 470 MPa $\sqrt{m}$, respectively. Figure 4 shows that the stress intensity factor remains constant at some stages of dike propagation, indicating steady state propagation. For example, K_I is nearly a constant of about 130 MPa $\sqrt{m}$ over
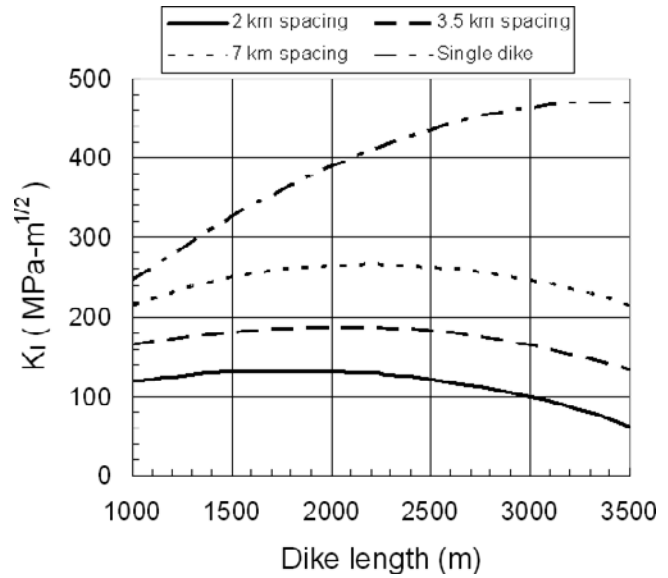
a range of dike length from 1300 m to 2200 m for the parallel dikes with a spacing of 2 km. For the case of an increased dike spacing of 3.5 km, K_I remains nearly constant but the value is about 185 MPa $\sqrt{m}$ over a range of dike length from 1500 m to 2500 m. Using the dike surface profile result, the dike surface area is approximately calculated as 3845 m² for the single dike. The area reduces to 519 m² for an individual dike in the multiple dike system with 2 km spacing.

[24] Figures 6 and 7 show the stress intensity factor versus dike length and the dike surface profiles, respectively, for the dikes that have grown to a length of 5 km. The magma
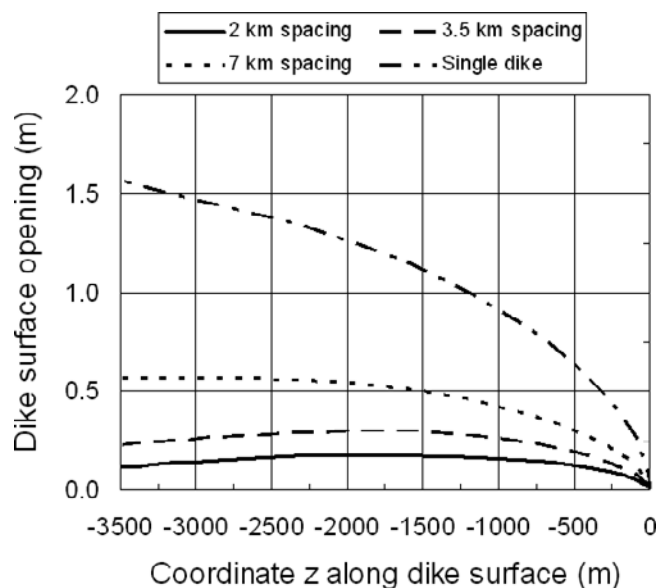
Figure 5. The dike surface opening displacement when the magma source region is 3.5 km below the LNB (V = 0.01 m/s, $\Delta\rho_0$ = 210 kg/m³).
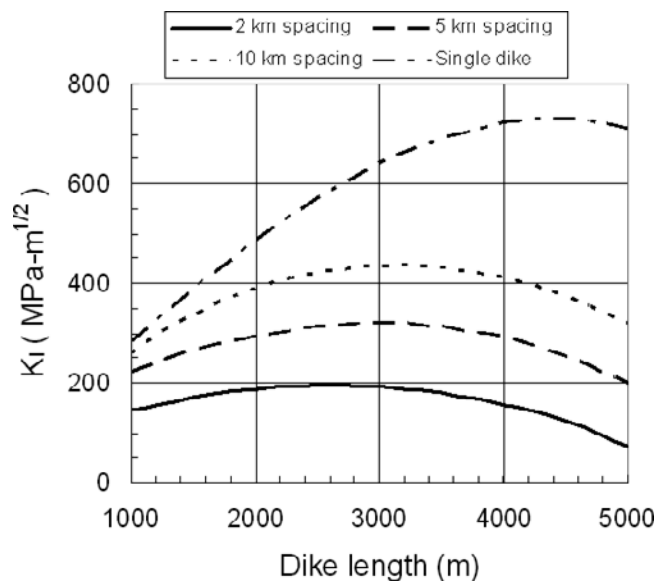
Figure 6. The stress intensity factor versus dike length when the magma source region is 5 km below the LNB (V = 0.01 m/s, $\Delta\rho_0$ = 300 kg/m³).

Figure 7. The dike surface opening displacement when the magma source region is 5 km below the LNB (V = 0.01 m/s, $\Delta\rho_0$ = 300 kg/m³).

source region is now assumed to be 5 km below the LNB. The density difference $\Delta\rho_0$ at the dike base is 300 kg/m³. Dike spacing of 2 km, as well as illustrative spacings of 5 km and 10 km are selected. The other parameters remain the same as those in Figures 2 and 3. The trends in stress intensity factor and dike surface displacement again are similar to those shown in Figures 2 and 3, respectively. The stress intensity factors become even larger because of the longer dike length and the higher buoyancy force. The peak K_I value for the 2 km spacing multiple dikes is about 196 MPa $\sqrt{m}$. The corresponding peak K_I values for the 5 km and 10 km spacing dikes, and the single dike are about 320, 437, and 730 MPa $\sqrt{m}$, respectively. Using the dike surface profile result, the dike surface area is approximately calculated as 10224 m² for the single dike. For an individual dike in the multiple dike system with 2 km spacing, the area reduces to 989 m² which is less than 10% of that for the single dike model.

[25] Figure 8 shows the stress intensity factor versus propagation velocity at a dike length of a = 5 km for the 5 km spacing parallel dikes. It is observed that K_I decreases significantly with increasing propagation velocity. The stress intensity factor is about 200 MPa $\sqrt{m}$ at a dike propagation velocity of 0.01 m/s and reduces to about 92 MPa $\sqrt{m}$ when the dike propagation velocity increases to 0.1 m/s.

5. Fracture Toughness of Crustal Rocks

[26] Fracture toughness represents a material's resistance to crack propagation. Fracture toughness is a constant for a perfect brittle material, but a function of crack extension for a material with some energy dissipation mechanisms (e.g., microcracking and plasticity). In the latter case, an effective fracture toughness concept may be adopted [*Rivalta and Dahm*, 2004, 2006]. When a crack propagates, the stress intensity factor at the crack tip equals the fracture tough-

ness. It is well known that the measured fracture toughness of rocks under atmospheric pressure is on the order of 1 MPa $\sqrt{m}$ [*Scholz*, 2002]. The existing solutions for the propagation of a single dike indicate that the stress intensity factor at the dike tip may attain a value on the order of 1000 MPa $\sqrt{m}$ (cf. Figure 6). It has been suggested that these unusually high fracture toughness values result from the energy dissipations (e.g., microcracking and plasticity) in the tip region of long dikes [*Heimpel and Olson*, 1994]. However, fracture toughness enhancements in brittle materials such as ceramics and rocks due to the crack tip process zone under atmospheric pressure are usually less than 10 MPa $\sqrt{m}$ [*Wachtman*, 1996]. High confining pressures at mantle and crustal conditions are also believed to contribute to the high
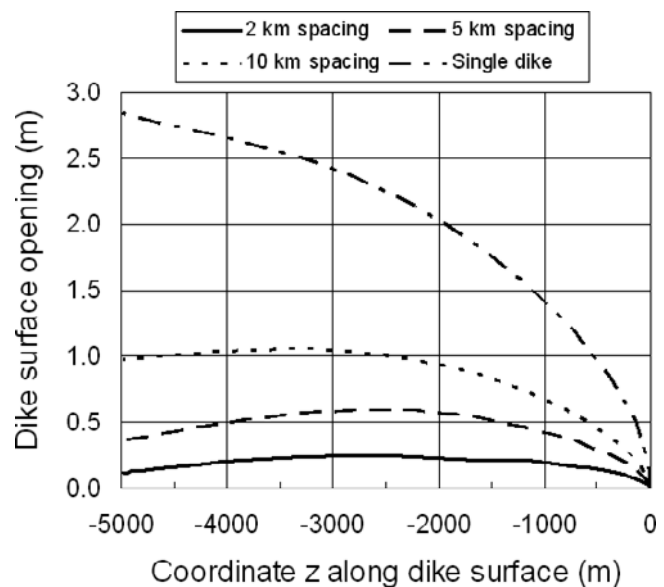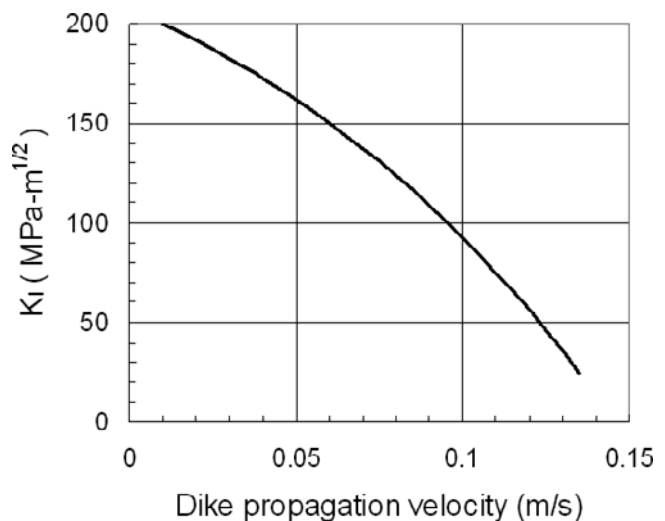
Figure 8. The stress intensity factor versus propagation velocity when the magma source region is 5 km below the LNB (a = 5 km, H = 5 km, $\Delta\rho_0$ = 300 kg/m³).

fracture toughness values. Some experimental investigations on the fracture toughness of sandstone under high confining pressures show that the toughness increases to 10 MPa $\sqrt{m}$ when the confining pressure increases to 100 MPa [*Winter*, 1983; *Terrien et al.*, 1983]. If the trend of the fracture toughness versus confining pressure relation persists to 1 GPa, which may typify lower crust/upper mantle depths, extrapolation of the test data of *Winter* [1983] would give an effective fracture toughness on the order of 100 MPa $\sqrt{m}$, which is one order of magnitude smaller than the predictions from the propagation of a single dike. For typical over pressure of 3 MPa and dike propagation velocity of 0.01 m/s, the present analyses using the parallel dike model with 2 km spacing (based on the dike patterns in the Oman ophiolite, *Nicolas et al.* [1994]) yield the peak stress intensity factors (steady state values) of about 92, 132 and 196 MPa $\sqrt{m}$ for the magma source located 2, 3.5 and 5 km below the LNB, respectively. These stress intensity factors on the order of 100 MPa $\sqrt{m}$ are much smaller than that inferred from the propagation of a single dike. In other words, the parallel dikes modeled here could not propagate simultaneously if host rock fracture toughness values are on the order of 1000 MPa $\sqrt{m}$. This finding is further supported by a number of field-based estimates of fracture toughness values of crustal rocks. For example, *Delaney and Pollard* [1981] estimated fracture toughness values in the range between 50 to 150 MPa $\sqrt{m}$ using the observed dike geometry. The estimates of *Parfitt* [1991] fall in the range of 30–110 MPa $\sqrt{m}$. *Rivalta and Dahm* [2006] experimentally estimated the fracture toughness of a rising dike from hypocenter migration and also reached a value of about 100 MPa $\sqrt{m}$. We note that the precise determination of fracture toughness requires knowledge of a number of physical parameters including overpressure, dike propagation velocity, modulus of rock, densities of rock and magma, and magma viscosity. Tectonic stress also plays a role as it influence the net pressure on the dike surfaces. A higher overpressure increases dike tip stress intensity factor, whereas a higher propagation velocity results in a lower stress intensity factor.

6. Concluding Remarks

[27] We have obtained the solutions of stress intensity factor and dike surface profile for the propagation of an array of periodic dikes propagating from a magma chamber or zone of partial melt into a semi-infinite elastic medium. The stress intensity factor at the tips of the multiple dikes is significantly smaller than that for a single dike propagation under otherwise the same conditions. Using typical physical parameters for mafic dike injection, the present analyses using the parallel dike model with 2 km spacing yield the peak stress intensity factors (steady state values) of about 92, 132 and 196 MPa $\sqrt{m}$ for the magma source located 2, 3.5 and 5 km below the LNB, respectively. These results imply that the fracture toughness of host rocks at depths approximately from the LNB to 5 km below the LNB may be on the order of 100 MPa $\sqrt{m}$ instead of the 1000 MPa $\sqrt{m}$ inferred from the propagation of a single dike if it is assumed that the stress intensity factor equals the fracture toughness during dike propagation.

[28] The value of stress intensity factor at a propagating dike tip may be regarded as an effective fracture toughness of the host rock, which includes the effect of the cohesive energy related to the damage in the dike tip region and thus may vary with dike propagation. The stress intensity factor values presented here are in agreement with some field-based estimates [*Delaney and Pollard*, 1981; *Parfitt*, 1991; *Rivalta and Dahm*, 2006]. In addition to the reduced stress intensity factors for multiple dikes, the dike surface opening displacement also decreases, which results in higher magma pressure gradients in multiple dikes and smaller volume of magma transport through dikes.

[29] The numerical results show that small dike spacing may significantly reduce the propagation velocity for multiple dikes. Dikes traveling at very low velocity may be arrested due to the solidification of magma [see, e.g., *Lister*, 1994a, 1994b; *Rubin*, 1995b; *Bolchover and Lister*, 1999], which is not considered in the present study. Further investigations require a coupling approach to take into account both magma flow and solidification, and non-periodic spacing of dikes with different lengths.

[30] The present solution of steady state propagation may be approximately applicable to some stages of dike propagation during which the effects of density gradation and overpressured source trade off and the calculated stress intensity factor remains constant. The steady state solution, however, may be employed to delineate the effect of dike spacing on the dike propagation and magma transport behavior. Furthermore, the solution may also be used to estimate the order of magnitude of fracture toughness of crustal rocks in a confining pressure environment because the steady state stress intensity factor corresponds to the maximum fracture toughness of the material.

References

Anderson, T. L. (1991), *Fracture Mechanics: Fundamentals and Applications*, CRC Press, Boca Raton.
Bahr, H. A., G. Fischer, and H. J. Weiss (1986), Thermal shock crack patterns explained by single and multiple crack propagation, *J. Mater. Sci.*, *21*, 2716–2720.
Benthem, J. P., and W. T. Koiter (1973), Asymptotic approximations to crack problems, in *Mechanics of Fracture*, Vol. 1: *Methods of Analysis and Solutions of Crack Problems*, edited by G. C. Sih, pp. 131–178, Noordhoff International Publishing, Leyden, The Netherlands.
Babiker, M., and A. Gudmundsson (2004), Geometry, structure and emplacement of mafic dykes in the Red Sea Hills, Sudan, *J. Afr. Earth Sci.*, *38*, 279–292.
Bolchover, P., and J. R. Lister (1999), The effect of solidification on fluid-driven fracture, *Proc. R. Soc. Ser. A and Ser. B*, *A455*, 2389–2409.
Bonafede, M., and M. Olivieri (1995), Displacement and gravity anomaly produced by a shallow vertical dike, *Geophys. J. Int.*, *123*, 639–652.
Bonafede, M., and E. Rivalta (1999), On tensile cracks close to and across the interface between two welded elastic half-space, *Geophys. J. Int.*, *138*, 410–434.
Canon-Tapia, E., and O. Merle (2006), Dyke nucleation and early growth from pressurized magma chambers: Insights from analogue models, *J. Volcanol. Geotherm. Res.*, *158*, 207–220.
Chen, Z., Z.-H. Jin, and S. E. Johnson (2007), A perturbation solution for dike propagation in an elastic medium with graded density, *Geophys. J. Int.*, *169*, 348–356.
Clemens, J. D., and C. K. Mawer (1992), Granitic magma transport by fracture propagation, *Tectonophysics*, *204*, 339–360.

Dahm, T. (2000a), Numerical simulations of the propagation and arrest of fluid-filled fractures in the Earth, *Geophys. J. Int.*, 141, 623–638.

Dahm, T. (2000b), On the shape and velocity of fluid-filled fractures in the Earth, *Geophys. J. Int.*, 142, 181–192.

Delaney, P. T., and D. D. Pollard (1981), Deformation of host rocks and flow of magma during growth of minette dikes and Breccia-bearing intrusions near Ship Rock, New Mexico, *USGS Prof. Pap.*, 1202.

Ernst, R. E., E. B. Grosfils, and D. Mege (2001), Giant dike swarms: Earth, Venus and Mars, *Annu. Rev. Earth Planet. Sci.*, 29, 489–534.

Ernst, R. E., K. L. Buchan, and I. H. Campbell (2005), Frontiers in Large Igneous Province research, *Lithos*, 79, 271–297.

Fialko, Y. A., and A. M. Rubin (1998), Thermodynamics of lateral dike propagation: Implications for crustal accretion at slow spreading mid-ocean ridges, *J. Geophys. Res.*, 103(B2), 2501–2514.

Geyer, J. F., and S. Nemat-Nasser (1982), Experimental investigation of thermally induced interacting cracks in brittle solids, *Int. J. Solids Struct.*, 18, 349–356.

Gudmundsson, A. (1983), Form and dimensions of dykes in eastern Iceland, *Tectonophysics*, 95, 295–307.

Gudmundsson, A. (1990), Dyke emplacement at divergent plate boundaries, in A. J. Parker, P. C. Rickwood, D. H. Tucker (Eds.), *Mafic dykes and emplacement mechanisms*, Balkema, Rotterdam, pp. 47–62.

Gudmundsson, A. (1995), Infrastructure and mechanics of volcanic systems in Iceland, *J. Volcanol. Geotherm. Res.*, 64, 1–2.

Gudmundsson, A. (2006), How local stresses control magma-chamber ruptures, dyke injections, and eruptions in composite volcanoes, *Earth Sci. Rev.*, 79, 1–31.

Guernina, S., and E. W. Sawyer (2003), Large-scale melt-depletion in granulite terranes: An example from the Archean Ashuanipi Subprovince of Quebec, *J. Metamorph. Geol.*, 21, 181–201.

Halls, H. C., and W. F. Fahrig (Eds.) (1987), Mafic Dyke Swarms, Special Paper: Toronto, Geological Association of Canada, 503 p.

Heimpel, M., and P. Olson (1994), Buoyancy-driven fracture and magma transport through the lithosphere, in *Magmatic Systems*, edited by M. P. Ryan, pp. 223–240, Academic, San Diego, CA.

Ida, Y. (1999), Effects of the crustal stress on the growth of dikes: Conditions of intrusion and extrusion of magma, *J. Geophys. Res.*, 104(B8), 17,897–17,909.

Ito, G., and S. J. Martel (2002), Focusing of magma in the upper mantle through dike interaction, *J. Geophys. Res.*, 107(B10), 2223, doi:10.1029/2001JB000251.

Johnson, S. E., S. R. Paterson, and M. C. Tate (1999), Structure and emplacement history of a multiple-center, cone-sheet-bearing ring complex: The Zarza Intrusive Complex, Baja California, México, *Bull. Geol. Soc. Am.*, 111, 607–619.

Kelemen, P. B., G. Hirth, N. Shimizu, M. Spiegelman, and H. J. B. Dick (1997), A review of melt migration processes in the adiabatically upwelling mantle beneath oceanic spreading ridges, *Philos. Trans. R. Soc. Ser. A and Serv. B*, 355, 283–318.

Kuhn, D., and T. Dahm (2004), Simulation of magma ascent by dykes in the mantle beneath mid-ocean ridges, *J. Geodyn.*, 38, 147–159.

Lister, J. R. (1990), Buoyancy-driven fluid fracture: the effects of material toughness and of low-viscosity precursors, *J. Fluid Mech.*, 210, 263–280.

Lister, J. R. (1991), Steady solutions for feeder dikes in a density-stratified lithosphere, *Earth Planet. Sci. Lett.*, 107, 233–242.

Lister, J. R. (1994a), The solidification of buoyancy-driven flow in a flexible-walled channel, Part 1 Constant-volume release, *J. Fluid Mech.*, 272, 21–44.

Lister, J. R. (1994b), The solidification of buoyancy-driven flow in a flexible-walled channel, Part 2 Continual release, *J. Fluid Mech.*, 272, 45–65.

Lister, J. R., and R. C. Kerr (1991), Fluid-mechanical models of crack propagation and their application to magma transport in dikes, *J. Geophys. Res.*, 96(B6), 10,049–10,077.

McLeod, P., and S. Tait (1999), The growth of dykes from magma chambers, *J. Volcanol. Geotherm. Res.*, 92, 231–246.

Menand, T., and S. R. Tait (2002), The propagation of a buoyant liquid-filled fissure from a source under constant pressure: An experimental approach, *J. Geophys. Res.*, 107(B11), 2306, doi:10.1029/2001JB000589.

Meriaux, C., and C. Jaupart (1998), Crack propagation through an elastic plate, *J. Geophys. Res.*, 103(B8), 18,295–18,314.

Meriaux, C., J. R. Lister, V. Lyakhovsky, and A. Agnon (1999), Dyke propagation with distributed damage of the host rock, *Earth Planet. Sci. Lett.*, 165, 177–185.

Nakajima, J., T. Matsuzawa, and A. Hasegawa (2001), Three dimensional structure of Vp, Vs, and Vp/Vs beneath northeaster Japan: Implications for arc magmatism and fluids, *J. Geophy. Res.*, 106(B10), 21,843–21,857.

Nicolas, A., F. Boudier, and B. Ildefonse (1994), Dike patterns in diapirs beneath oceanic ridges: the Oman ophiolite, in *Magmatic Systems*, edited by M. P. Ryan, pp. 77–95, Academic, San Diego, CA.

Nied, H. F. (1987), Periodic array of cracks in half-plane subjected to arbitrary loading, *ASME J. Appl. Mech.*, 54, 642–648.

Panton, R. L. (1984), *Incompressible Flow*, John Wiley & Sons, New York.

Parfitt, E. A. (1991), The role of rift zone storage in controlling the site and timing of eruptions and intrusions at Kilauea Volcano, Hawaii, *J. Geophys. Res.*, 96, 10,101–10,112.

Parfitt, E. A., and J. W. Head III (1993), Buffered and unbuffered dike emplacement on Earth and Venus: Implications for magma reservoir size, depth, and rate of magma replenishment, *Earth Moon Planets*, 61, 249–281.

Pollard, D. D. (1987), Elementary fracture mechanics applied to the structural interpretation of dikes, in *Mafic Dike Swarms*, edited by H. C. Halls and W. H. Fahrig, pp. 5–24, Geological Association of Canada Special Paper 34.

Ray, R., H. C. Sheth, and J. Mallik (2007), Structure and emplacement of the Nandurbar-Dhule makic dyke swarm, Deccan Traps, and the tectonomagmatic evolution of flood basalts, *Bull. Volcanol.*, 69, 537–551.

Rivalta, E., and T. Dahm (2004), Dyke emplacement in fractured media: Application to the 2000 intrusion at Izu islands, Japan, *Geophys. J. Int.*, 157, 283–292.

Rivalta, E., and T. Dahm (2006), Acceleration of buoyancy-driven fractures and magmatic dikes beneath the free surface, *Geophys. J. Int.*, 166, 1424–1439.

Roper, S. M., and J. R. Lister (2005), Buoyancy-driven crack propagation from an over-pressure source, *J. Fluid Mech.*, 536, 79–98.

Rubin, A. M. (1993), Dikes vs. diapirs in viscoelastic rock, *Earth Planet. Sci. Lett*, 119, 641–659.

Rubin, A. M. (1995a), Propagation of magma-filled crack, *Annu. Rev. Earth Planet. Sci*, 23, 287–3336.

Rubin, A. M. (1995b), Getting granite dikes out of the source region, *J. Geophys. Res.*, 100(B4), 5911–5929.

Rubin, A. M. (1998), Dike ascent in partially molten rock, *J. Geophys. Res.*, 103(B9), 20,901–20,919.

Ryan, M. P. (1994), Neutral-buoyancy controlled magma transport and storage in mid-ocean ridge magma reservoirs and their sheeted-dike complex: a summary of basic relationships, in *Magmatic Systems*, edited by M. P. Ryan, pp. 97–138, Academic, San Diego, CA.

Secor, D., and D. Pollard (1975), On stability of open hydraulic fractures in the Earth's crust, *Geophys. Res. Lett.*, 2, 510–513.

Segall, P., P. Cervelli, S. Owen, M. Lisowski, and A. Miklius (2001), Constraints on dike propagation from continuous GPS measurements, *J. Geophys. Res.*, 106(B9), 19,301–19,317.

Scholz, C. H. (2002), *The Mechanics of Earthquakes and Faulting*, Second edition, Cambridge University Press, Cambridge, UK.

Spence, D. A., and P. Sharp (1985), Self-similar solutions for elastohydro-dynamic cavity flow, *Proc. R. Soc. Ser. A and Ser. B*, A400, 289–313.

Spence, D. A., P. Sharp, and D. L. Turcotte (1987), Buoyancy-driven crack propagation: A mechanism for magma migration, *J. Fluid Mech.*, 174, 135–153.

Takada, A. (1989), Magma transport and reservoir formation by a system of propagating cracks, *Bull. Volcanol.*, 52, 118–126.

Takada, A. (1994), Accumulation of magma in space and time by crack interaction, in *Magmatic Systems*, edited by M. P. Ryan, pp. 241–257, Academic, San Diego, CA.

Terrien, M., J. P. Sarda, M. Chayed'Albissin, and J. Berges (1983), Experimental study of the anisotropiy of a sandstaone and a marble (abstract), in *Int. Congress CNRS 351. Failure Criteria of Structured Media*, Villard le Lans.

Unsworth, M. J., A. G. Jones, W. Wei, G. Marquis, S. G. Gokarn, and J. E. Spratt (2005), Crustal rheology of the Himalaya and Southern Tibet inferred from magnetotelluric data, *Nature*, 438, 78–81.

Wachtman, J. B. (1996), *Mechanical Properties of Ceramics*, Wiley, New York.

Walker, G. P. L. (1986), Koolau dike complex, Oahu: Intensity and origin of a sheeted-dike complex high in an Hawaiian volcanic edifice, *Geology*, 14, 310–313.

Weertman, J. (1971), Theory of water-filled crevasses in glaciers applied to vertical magma transport beneath oceanic ridges, *J. Geophys. Res.*, 76, 1171–1183.

Winter, R. B. (1983), *Berichte vom Institut fur Geophysik*, Reihe A, Nr. 13. Ruhr-Universitat, Bochum.

Wright, T. L., and F. W. Klein (2006), Deep magma transport at Kiluea volcano, Hawaii, *Lithos*, 87, 50–79.

Yamaoka, K., M. Kawamura, F. Kimata, N. Fujii, and T. Kudo (2005), Dike intrusion associated with the 2000 eruption of Miyakejima Volcano, Japan, *Bull. Volcanol.*, 67, 231–242.

—————————

Z.-H. Jin, Department of Mechanical Engineering, University of Maine, Orono, ME 04469, USA. (zhihe.jin@maine.edu)

S. E. Johnson, Department of Earth Sciences, University of Maine, Orono, ME 04469, USA.